Probabilistic Active Distribution Network Equivalence with Correlated Uncertain Injections

Bin Huang, Zhigang Li, *Member, IEEE*, J.H. Zheng, *Member, IEEE*, and Q. H. Wu, *Fellow, IEEE*

***Abstract*—Equivalent modeling for active distribution network (ADN) is essential to improve the efficiency of analyzing the transmission network. The currently available equivalent modeling methods for ADN neglect the probabilistic characteristics of renewable energy sources (RES). To tackle this issue, this paper proposes a probabilistic equivalent modeling method (PEMM) for ADN considering the uncertainty of RES. In the proposed method, the uncertainty of RES is reflected in the equivalent boundary bus injection using the cumulant analysis based on the approximate linearization of ADN. PEMM is extended to incorporate the correlation of RES through the orthogonal transformation. A sampling method using Gaussian copula function is employed to generate the correlated samples and the joint cumulants, providing the input data for PEMM. The results of case studies demonstrate the effectiveness of PEMM and verify that the involvement of correlation can improve the accuracy of PEMM.**

***Index Terms*—Active distribution network, correlation, cumulant, equivalent modeling, uncertainty**

I. Introduction

DUE to the increasing appeal to the utilization of clean energy, the large-scale renewable energy sources (RES) are integrated into the distribution network [1]. Nowadays, the distribution network gradually turns into the active distribution network (ADN), which may supply the surplus power for the transmission network when RES is abundant. Hence, the analysis of the coupled transmission and distribution system (CTDS) must consider the impact of the RES. From the perspective of transmission system operators (TSOs), it is impractical and unnecessary to analyze the transmission side using the detailed model of ADNs for two reasons. First, the scale and complexity of the ADN will impair the efficiency of the analysis procedure. Second, TSOs and distribution system operators (DSOs) usually function independently, which means that the detailed information of them is commercially sensitive and not transparent to each other. As an essential tool to analyze the transmission network considering the impact of the RES, the equivalent methods for ADN has recently attracted the attention of researchers. The main goal of these equivalent methods is to construct the equivalent model of ADN, which can preserve the behaviours of ADN while keeping the structure and the mathematical model as simple as possible.

Because ADN is characterized by the penetration of RES, the modeling of the renewable power generation is critical to the equivalence of ADN. To conduct the dynamic analysis, [2] and [3] use an equivalent converter-connected synchronous generator to represent the distributed generators (DGs) in ADN. In [4], the photovoltaic (PV) generation systems embedded with voltage support schemes in ADN are aggregated to a separate equivalent PV generator which preserves the voltage support schemes. In [5], the equivalent model for DGs is derived from the numerical approach, in which the reactive power output and the inverter power loss of the DGs are considered. References [6] and [7] adopt an equivalent generator to represent the DGs in ADN and the nodes with DGs connected in ADN are regarded as either PQ nodes or PV nodes. The aforementioned references [2]–[8] ignore the uncertainty of the DGs of RES. In fact, uncertainty is the inherent property of RES due to climatic conditions. In terms of the economic dispatch, neglecting the uncertainty of RES may result in the untrustworthy operation schedule and thus the operators may have to deploy excessive reserve capacity [9]. Besides, taking the uncertainty into account can help operators to obtain a better solution to long-term planning and congestion management. Thus, the equivalent model for ADN should take the uncertainty of the RES into account, so as to provide the model for further research and analysis.

Except for the uncertain property, another vital feature of RES is the correlation. Since the regional scope of ADN is usually small and the meteorological condition within ADN is similar, the wind power generation in different wind farms in ADN is correlated [10], so is the PV generation in different PV plants. Ignoring the correlation can lead to the biases in the analysis results of the system, resulting in higher operating costs and higher risks to the stability of power system [11]. Hence, the equivalent model for ADN should consider the correlation of RES. Reference [12] uses Cholesky decomposition to generate the correlated variables which only represent the linear correlation. Reference [10] uses the copula function to describe the non-linear correlation. However, when using the copula function to handle the correlation, few references investigate the derivation of the joint cumulants, which are the essential quantities towards joint probability distribution.

To summarize, few studies have considered the uncertainty of RES when developing the equivalent model for ADN despite the uncertainty of RES is essential in the analysis and optimization of CTDS. In addition, the correlation of RES is seldom discussed in the currently available equivalent modeling method. To bridge these gaps, the contributions of this paper are summarized as follows:

(1) A probabilistic equivalent modeling method (PEMM) is proposed to obtain the probabilistic equivalent model of ADN. The uncertain property of RES is preserved and

The authors are with School of Electric Power Engineering, South China University of Technology, Guangzhou, 510641, China (lizg16@scut.edu.cn).

aggregated to the boundary bus using the properties of cumulant and the approximately linear relationship between the equivalent boundary power injection and the internal power injection in ADN.

(2) PEMM is formulated to incorporate the correlated power injection through the orthogonal transformation, which can extend the scope of PEMM to the equivalent modeling of ADN with the correlated RES embedded.

(3) With the copula function, a sampling method is used to generate the correlated samples and the joint cumulants, which serve as the input data for PEMM to build a more accurate probabilistic equivalent model for ADN.

The rest of this paper is organized as follows. Stochastic injection in ADN is formulated in Section II. In Section III, PEMM for ADN is proposed and extended to incorporate the correlated power generation of RES. A sampling method to generate the correlated samples and the joint cumulants using the copula function is also proposed in Section III. In Section IV, case studies are taken to evaluate the performance of the proposed modeling method. Finally, conclusions are given in Section V.

II. Stochastic Injection Modeling in ADN

Active distribution network (ADN) is characterized by high penetration of RES, which is inherently stochastic due to the natural condition. Besides, the loads in ADN are uncertain due to predictive errors and their inherent stochastic characteristic. In this section, the uncertain of the power injection of ADN is described. The model of PVs is presented firstly, followed by the model of wind power and load.

A. Model of PVs

Typically, ADN is equipped with PV plants to supply usable solar power. Beta distribution is used to model the uncertainty of solar irradiance [13]:

$$f_{\mathrm{r}}(r)=\begin{cases}\dfrac{\Gamma(\alpha+\beta)}{\Gamma(\alpha)+\Gamma(\beta)}(\dfrac{r}{r_{\max}})^{\alpha-1}(1-\dfrac{r}{r_{\max}})^{\beta-1} & \\ \qquad 0\le r\le r_{\max},\alpha\ge 0,\beta\ge 0 & \\ 0 \qquad\qquad r\le 0 \quad \text{or} \quad r\ge r_{\max} & \end{cases}, \tag{1}$$

where r and $r_{\max}$ are the solar irradiance and maximum solar irradiance, respectively. α and β are the function parameters, and Γ represents the Γ function.

Accordingly, the PDF of the active power output of PV plant is formulated as:

$$f_{\mathrm{pv}}(P_{\mathrm{pv}})=\frac{\Gamma(\alpha+\beta)}{\Gamma(\alpha)+\Gamma(\beta)}(\frac{P_{\mathrm{pv}}}{P_{\mathrm{pv,max}}})^{\alpha-1}(1-\frac{P_{\mathrm{pv}}}{P_{\mathrm{pv,max}}})^{\beta-1}, \tag{2}$$

$P_{\mathrm{pv,max}}$ is the maximum active power output of the PV plant:

$$P_{\mathrm{pv,max}}=A\eta_{\mathrm{pv}}r_{\max}, \tag{3}$$

where η_{pv} is the comprehensive conversion efficiency of PV plant and A is the areas of the PV cells within one PV plant.

With the capacitor compensator and the control strategies used in the PV plant, the reactive power output of PV plant Q_{pv} is proportional to the P_{pv}.

B. Model of Wind Power

Weibull distribution is commonly used to describe the probabilistic property of wind speed [10]:

$$f_{\mathrm{w}}(x)=\begin{cases}\dfrac{k}{\lambda}(\dfrac{x}{\lambda})^{k-1}\exp(-(\dfrac{x}{\lambda})^{k}) & x\ge 0\\ 0 & x\le 0\end{cases}, \tag{4}$$

where x is the wind speed, k is the shape parameter of the distribution , λ is the scale parameter of the distribution.

Relationship between the wind speed and the output power of a wind farm is formulated as [10]:

$$P_{\mathrm{w}}(v)=\begin{cases}0, & v\le v_{\mathrm{ci}}, v\ge v_{\mathrm{co}}\\ P_{\mathrm{N}}, & v_{\mathrm{N}}\le v\le v_{\mathrm{co}}\\ g(v), & v_{\mathrm{ci}}\le v\le v_{\mathrm{N}}\end{cases}, \tag{5}$$

where v_{ci}, v_{co}, and v_{N} are the cut-in, cut-out, and the nominal wind speed, respectively; $g(v)$ is the function which describes the relationship between the power output and the wind speed in the interval of wind speed $[v_{\mathrm{ci}}, v_{\mathrm{N}}]$ and can be expressed as:

$$g(v)=\frac{1}{2}\pi\rho C_p(\lambda,\beta)R^2v^3, \tag{6}$$

where ρ is the air density (typically 1.25 km/m^3), β is the pitch angle (in degrees), R is the blade radius (in meters), $C_p(\lambda,\beta)$ is the wind-turbine power coefficient.

Similar to PV plant, the reactive power generated by a wind farm can be calculated as:

$$Q_{\mathrm{w}}=P_{\mathrm{w}}\sqrt{1-\cos^2\varphi}/\cos\varphi, \tag{7}$$

where $\cos\varphi$ is the power factor of the wind farm.

C. Load

Considering the time-varying and uncertain characteristic of load, the normal distribution is commonly used to describe the active power load uncertainty [13], [14]:

$$f_l(P_{\mathrm{l}})=\exp(-\frac{(P_{\mathrm{l}}-\mu_{p_{\mathrm{l}}})^2}{2\sigma_{p_{\mathrm{l}}}^2})/\sqrt{2\pi}\sigma_{p_{\mathrm{l}}}, \tag{8}$$

where $f(P_{\mathrm{l}})$ is the PDF of active power load; $\mu_{p_{\mathrm{l}}}$ and $\sigma_{p_{\mathrm{l}}}$ are the mean and standard derivation of the active power load, respectively.

The PDF of reactive power load can be similarly derived.

III. Probabilistic Equivalent Modeling of ADN

Generally, the transmission and distribution systems are interconnected via the boundary bus, as illustrated in Fig. 1. To enhance the efficiency of analysis upon the transmission system, the goal of PEMM is to replace the ADN with the equivalent boundary power injection, which can retain the consistency of load flow and the consistency of probabilistic characteristics of RES in ADN.

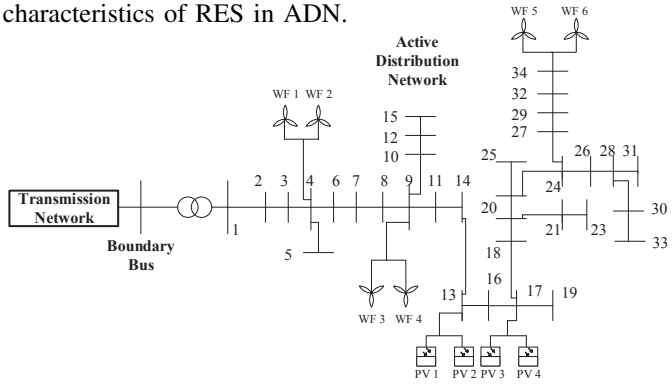

Fig. 1. An illustrative example of the CTDS.

A. Approximate Linearization

The nodal voltage equations of the CTDS can be expressed in matrix form:

$$\begin{bmatrix} \boldsymbol{Y}_{\mathrm{EE}} & \boldsymbol{Y}_{\mathrm{EB}} & \\ \boldsymbol{Y}_{\mathrm{BE}} & \boldsymbol{Y}_{\mathrm{BB}} & \boldsymbol{Y}_{\mathrm{BI}} \\ & \boldsymbol{Y}_{\mathrm{IB}} & \boldsymbol{Y}_{\mathrm{II}} \end{bmatrix} \begin{bmatrix} \dot{\boldsymbol{V}}_{\mathrm{E}} \\ \dot{\boldsymbol{V}}_{\mathrm{B}} \\ \dot{\boldsymbol{V}}_{\mathrm{I}} \end{bmatrix} = \begin{bmatrix} \dot{\boldsymbol{I}}_{\mathrm{E}} \\ \dot{\boldsymbol{I}}_{\mathrm{B}} \\ \dot{\boldsymbol{I}}_{\mathrm{I}} \end{bmatrix}, \tag{9}$$

where $\boldsymbol{Y}$ is the bus admittance matrix, $\dot{\boldsymbol{V}}$ is the nodal voltage vector, $\dot{\boldsymbol{I}}$ is the nodal current injection vector and subscript E, B, I denote the element of matrix and vector corresponding to the buses of ADN, the boundary buses and the buses of the transmission network, respectively.

By performing the Gaussian elimination on (9) to eliminate $\dot{\boldsymbol{V}}_{\mathrm{E}}$ and transforming nodal current injection into nodal power injection, the nodal voltage equations of the boundary buses in the equivalent network are expressed as:

$$\begin{aligned} &(\boldsymbol{Y}_{\mathrm{BB}} - \boldsymbol{Y}_{\mathrm{BE}}{\boldsymbol{Y}_{\mathrm{EE}}}^{-1}\boldsymbol{Y}_{\mathrm{EB}})\dot{\boldsymbol{V}}_{\mathrm{B}} + \boldsymbol{Y}_{\mathrm{BI}}\dot{\boldsymbol{V}}_{\mathrm{I}} = \\ &(\mathrm{diag}[\dot{\boldsymbol{V}}_{\mathrm{B}}]^{-1})^{*}{\dot{\boldsymbol{S}}_{\mathrm{B}}}^{*} - \boldsymbol{Y}_{\mathrm{BE}}{\boldsymbol{Y}_{\mathrm{EE}}}^{-1}(\mathrm{diag}[\dot{\boldsymbol{V}}_{\mathrm{E}}]^{-1})^{*}{\dot{\boldsymbol{S}}_{\mathrm{E}}}^{*}, \end{aligned} \tag{10}$$

where $\dot{\boldsymbol{S}}$ is the nodal power injection, $()^{*}$ denotes the conjugate operator and diag$[*]$ is the diagonal operator.

Derived from (10), the equivalent boundary nodal power injection can be formulated as:

$$\Delta\dot{\boldsymbol{S}}_{\mathrm{B}} = -\mathrm{diag}[\dot{\boldsymbol{V}}_{\mathrm{B}}]\boldsymbol{Y}_{\mathrm{BE}}{\boldsymbol{Y}_{\mathrm{EE}}}^{-1}\mathrm{diag}[\dot{\boldsymbol{V}}_{\mathrm{E}}]^{-1}\dot{\boldsymbol{S}}_{\mathrm{E}}. \tag{11}$$

Hence, $\Delta\dot{\boldsymbol{S}}_{\mathrm{B}}$ is determined jointly by the $\boldsymbol{Y}_{\mathrm{BE}}{\boldsymbol{Y}_{\mathrm{EE}}}^{-1}$, $\dot{\boldsymbol{V}}_{\mathrm{B}}$, $\dot{\boldsymbol{V}}_{\mathrm{E}}$ and $\dot{\boldsymbol{S}}_{\mathrm{E}}$ at a base operating point. Assuming that $\boldsymbol{Y}_{\mathrm{BE}}{\boldsymbol{Y}_{\mathrm{EE}}}^{-1}$, $\dot{\boldsymbol{V}}_{\mathrm{B}}$ and $\dot{\boldsymbol{V}}_{\mathrm{E}}$ are constants at a given operating point, the equivalent boundary power injections $\Delta\boldsymbol{P}_{\mathrm{B}}$ and $\Delta\boldsymbol{Q}_{\mathrm{B}}$ are approximately linear to $\boldsymbol{P}_{\mathrm{E}}$ and $\boldsymbol{Q}_{\mathrm{E}}$:

$$\Delta\boldsymbol{P}_{\mathrm{B}} = \boldsymbol{E}_{\mathrm{P}}\boldsymbol{P}_{\mathrm{E}} + \boldsymbol{E}_{\mathrm{Q}}\boldsymbol{Q}_{\mathrm{E}}, \tag{12}$$

$$\Delta\boldsymbol{Q}_{\mathrm{B}} = -\boldsymbol{E}_{\mathrm{Q}}\boldsymbol{P}_{\mathrm{E}} + \boldsymbol{E}_{\mathrm{P}}\boldsymbol{Q}_{\mathrm{E}}, \tag{13}$$

where $\boldsymbol{E}_{\mathrm{P}}$, $\boldsymbol{E}_{\mathrm{Q}}$, $\boldsymbol{F}_{\mathrm{P}}$ and $\boldsymbol{F}_{\mathrm{Q}}$ are the coefficient as:

$$\begin{aligned} \boldsymbol{E}_{\mathrm{P}} &= \boldsymbol{C}_{\mathrm{B1}}\mathrm{diag}(|\boldsymbol{V}_{\mathrm{E}}|)^{-2}\boldsymbol{V}_{\mathrm{E,Re}} + \boldsymbol{C}_{\mathrm{B2}}\mathrm{diag}(|\boldsymbol{V}_{\mathrm{E}}|)^{-2}\boldsymbol{V}_{\mathrm{E,Im}}, \\ \boldsymbol{E}_{\mathrm{Q}} &= \boldsymbol{C}_{\mathrm{B1}}\mathrm{diag}(|\boldsymbol{V}_{\mathrm{E}}|)^{-2}\boldsymbol{V}_{\mathrm{E,Im}} - \boldsymbol{C}_{\mathrm{B2}}\mathrm{diag}(|\boldsymbol{V}_{\mathrm{E}}|^{-2}\boldsymbol{V}_{\mathrm{E,Re}}, \end{aligned} \tag{14}$$

$$\begin{aligned} \boldsymbol{C}_{\mathrm{B1}} &= \mathrm{diag}[\boldsymbol{V}_{\mathrm{B,Re}}](\boldsymbol{Y}_{\mathrm{BE}}{\boldsymbol{Y}_{\mathrm{EE}}}^{-1})_{\mathrm{Re}} \\ &\quad -\mathrm{diag}[\boldsymbol{V}_{\mathrm{B,Im}}](\boldsymbol{Y}_{\mathrm{BE}}{\boldsymbol{Y}_{\mathrm{EE}}}^{-1})_{\mathrm{Im}}, \\ \boldsymbol{C}_{\mathrm{B2}} &= \mathrm{diag}[\boldsymbol{V}_{\mathrm{B,Im}}](\boldsymbol{Y}_{\mathrm{BE}}{\boldsymbol{Y}_{\mathrm{EE}}}^{-1})_{\mathrm{Re}} \\ &\quad +\mathrm{diag}[\boldsymbol{V}_{\mathrm{B,Re}}](\boldsymbol{Y}_{\mathrm{BE}}{\boldsymbol{Y}_{\mathrm{EE}}}^{-1})_{\mathrm{Im}}, \end{aligned} \tag{15}$$

where $(*)_{\mathrm{Re}}$ and $(*)_{\mathrm{Im}}$ represent the real and imaginary part of $(*)$, respectively; $|*|$ denotes the magnitude of complex number.

Due to the emerging proliferation of the power generation from RES and the uncertain load, the nodal power injections of the ADN are stochastic. Traditional static equivalent technique, such as Ward equivalent and Radial Equivalent Independent, can only guarantee the consistency of load flow under specific operation states, without the consideration of maintaining the consistency of the probabilistic characteristics. Hence, they are not suitable for the equivalent modeling of ADN with uncertain injections.

B. Probabilistic Equivalence Using Cumulant

In this paper, a probabilistic equivalent modeling method using the cumulant is proposed to keep the consistency of both the load flow and the probabilistic characteristics together. The readers are referred to [15] for the basics of cumulants.

Let $\boldsymbol{\gamma}^{(v)}_{P\mathrm{g_E}}$ and $\boldsymbol{\gamma}^{(v)}_{P\mathrm{l_E}}$ be the v-th cumulants of the active power generation and the active power load in ADN, respectively. The definition of $\boldsymbol{\gamma}^{(v)}_{Q\mathrm{g_E}}$ and $\boldsymbol{\gamma}^{(v)}_{Q\mathrm{l_E}}$ are similar.

Supposed that the nodal power generation and the nodal load are independent, the v-th cumulants $\gamma^{(v)}_{P_{\mathrm{E}}}$ and v-th cumulants of reactive power injection $\gamma^{(v)}_{Q_{\mathrm{E}}}$ can be obtained using the additivity of cumulant:

$$\boldsymbol{\gamma}^{(v)}_{P_{\mathrm{E}}} = \boldsymbol{\gamma}^{(v)}_{P\mathrm{g_E}} + \boldsymbol{\gamma}^{(v)}_{P\mathrm{l_E}}, \boldsymbol{\gamma}^{(v)}_{Q_{\mathrm{E}}} = \boldsymbol{\gamma}^{(v)}_{Q\mathrm{g_E}} + \boldsymbol{\gamma}^{(v)}_{Q\mathrm{l_E}}. \tag{16}$$

After we obtain the $\boldsymbol{\gamma}^{(v)}_{P_{\mathrm{E}}}$ and $\boldsymbol{\gamma}^{(v)}_{Q_{\mathrm{E}}}$, we can deduce the expressions for the cumulants of equivalent boundary nodal power injections. For the sake of clarity, we first suppose that the nodal power injections in ADN are uncorrelated. According to (12) and (13) , the v-th cumulants of equivalent boundary nodal power injections can be deduced as:

$$\boldsymbol{\gamma}^{(v)}_{\Delta P_{\mathrm{B}}} = \boldsymbol{E}_{\mathrm{P}}{}^{\circ v}\boldsymbol{\gamma}^{(v)}_{P_{\mathrm{E}}} + \boldsymbol{E}_{\mathrm{Q}}{}^{\circ v}\boldsymbol{\gamma}^{(v)}_{Q_{\mathrm{E}}}, \tag{17}$$

$$\boldsymbol{\gamma}^{(v)}_{\Delta Q_{\mathrm{B}}} = -\boldsymbol{E}_{\mathrm{Q}}{}^{\circ v}\boldsymbol{\gamma}^{(v)}_{P_{\mathrm{E}}} + \boldsymbol{E}_{\mathrm{P}}{}^{\circ v}\boldsymbol{\gamma}^{(v)}_{Q_{\mathrm{E}}}, \tag{18}$$

where $[*]^{\circ v}$ is the Hadamard power operator.

It is noted that the derivation presented above take the advantage of the additivity and the homogeneity of the cumulant and the additivity relying on the condition that the stochastic variables are independent.

With $\boldsymbol{\gamma}^{(v)}_{\Delta P_{\mathrm{B}}}$ and $\boldsymbol{\gamma}^{(v)}_{\Delta Q_{\mathrm{B}}}$, the moments of equivalent boundary nodal power injection can be obtained using the relationship between cumulants and moments [15]. Thus, the probability characteristics of the power injections in ADN can be preserved and aggregated to the boundary buses. PEMM proposed in this paper utilizes the property of the cumulant to construct the probabilistic equivalent model, avoiding the complicated calculation of convolution. Compared with the original CTDS, the equivalent network obtained from PEMM is less complicated while still preserving the consistency of the probabilistic characteristic and the consistency of load flow.

C. Consideration of Correlation

The PEMM derived in section III-B does not consider the correlation of RES in the ADN. This section uses orthogonal transformation to incorporate the correlation into PEMM [16]. For convenience, we focus on discussing the correlation of active power generation.

Let $\boldsymbol{P}$ be the correlated active power injections vector in ADN:

$$\boldsymbol{P} = (p_1, p_2, \cdots, p_m), \tag{19}$$

with Pearson correlation coefficient matrix C_{p}.

$\boldsymbol{C}_{\mathrm{p}}$ is usually symmetric and also positive definite. Thus, Cholesky decomposition can be used to decompose $\boldsymbol{C}_{\mathrm{p}}$ [16]:

$$\boldsymbol{C}_{\mathrm{p}} = \boldsymbol{G}\boldsymbol{G}^{T}. \tag{20}$$

Then, the correlated active power injections $\boldsymbol{P}$ can be transformed into uncorrelated random variables $\boldsymbol{P}'$:

$$\boldsymbol{P}' = \boldsymbol{G}^{-1}\boldsymbol{P}. \tag{21}$$

Conversely, the corresponding inverse orthogonal transformation can be expressed as:

$$\boldsymbol{P} = \boldsymbol{G}\boldsymbol{P}'. \tag{22}$$

As formulated in (22), we can express the correlated v-th cumulants of nodal active power injection in ADN as the weighted linear combination of independent v-th cumulants using the inverse orthogonal transformation:

$$\gamma_{P_{\mathrm{E},j}}^{(v)} = \sum_{r=1}^{j} g_{jr}^{v} \gamma_{P'_{\mathrm{E},j}}^{(v)},\ j = 1, 2, \cdots, m, \tag{23}$$

where $\gamma_{P'_{\mathrm{E},j}}^{(v)}$ is the uncorrelated cumulant of active power injection in bus j of ADN , m is the number of buses of ADN, and g_{jr}^{v} is the j th row and r th column element of matrix $\boldsymbol{G}^{v}$.

By performing the orthogonal transformation, the correlated active power injections $\boldsymbol{P}$ can be transformed into uncorrelated random variables. Then, substituting (23) into (17) and (18) yields:

$$\gamma_{\Delta P_{\mathrm{B}}}^{(v)} = \tilde{\boldsymbol{E}}_{\mathrm{P}}{}^{\circ v} \gamma_{P'_{\mathrm{E}}}^{(v)} + \boldsymbol{E}_{\mathrm{Q}}{}^{\circ v} \gamma_{Q_{\mathrm{E}}}^{(v)}, \tag{24}$$

$$\gamma_{\Delta Q_{\mathrm{B}}}^{(v)} = -\tilde{\boldsymbol{E}}_{\mathrm{Q}}{}^{\circ v} \gamma_{P'_{\mathrm{E}}}^{(v)} + \boldsymbol{E}_{\mathrm{P}}{}^{\circ v} \gamma_{Q_{\mathrm{E}}}^{(v)}. \tag{25}$$

The elements of $\tilde{\boldsymbol{E}}_{\mathrm{P}}{}^{\circ v}$ and $\tilde{\boldsymbol{E}}_{\mathrm{Q}}{}^{\circ v}$ can be calculated by:

$$\tilde{e}_{\mathrm{p},ir}^{v} = \sum_{k=r}^{m} e_{\mathrm{p},ik}^{v}\ g_{kr}^{v},\ r = 1, 2, \cdots, m, \tag{26}$$

$$\tilde{e}_{\mathrm{q},ir}^{v} = \sum_{k=r}^{m} e_{\mathrm{q},ik}^{v}\ g_{kr}^{v},\ r = 1, 2, \cdots, m, \tag{27}$$

where $e_{\mathrm{p},ik}^{v}$ is the element of $\boldsymbol{E}_{\mathrm{P}}{}^{\circ v}$ in ith row and kth column, $e_{\mathrm{q},ik}^{v}$ is the element of $\boldsymbol{E}_{\mathrm{Q}}{}^{\circ v}$ in ith row and kth column; i is the index of the boundary buses and r is the index of the buses of ADN .

With (24) and (25), PEMM can take the correlation of active power injections in ADN into account. The similar procedure can be used to consider the correlated reactive power injections.

D. The Joint Cumulant of the Power Injection in ADN

When applying the PEMM for ADN, the first step is to obtain the cumulants of the power injections in ADN. In case that the outputs of wind farms and PV plants are correlated, the $\gamma_{P_{\text{pv, E}}}^{(v)}$, $\gamma_{P_{\text{wind, E}}}^{(v)}$, $\gamma_{Q_{\text{pv, E}}}^{(v)}$ and $\gamma_{Q_{\text{wind, E}}}^{(v)}$ are supposed to be the joint cumulants.

In the case that multiple PV plants or wind farms are integrated in a ADN, the probabilistic model for the renewable power generation is actually the multivariate distribution. However, it is intractable to obtain the joint probability distribution function for this multivariate distribution, and therefore it is difficult to obtain the joint cumulants directly [10].

Copula function can connect multiple univariate distributions to a multivariate distribution [17]. With marginal probability distributions for each random power injections and the correlation information such as Pearson correlation coefficient ρ, copula function can be used to connect these dispersive marginal probability distributions and to generate the samples of the correlated random variables.

In this section, we develop a sampling method to obtain the joint cumulants of the correlated renewable power generation using the copula function.

Sklar theorem states that any multivariate joint distribution $F(x_1, x_2, \cdots, x_N)$ can be expressed in the combination of N univariate marginal CDFs $F_1(x_1), F_2(x_2), \cdots, F_N(x_N)$ and a copula function $C(u_1, u_2, \cdots, u_N)$ defined in the N dimension space $[0, 1]^N$:

$$F(x_1, x_2, \cdots, x_N) = C(F_1(x_1), F_2(x_2), \cdots, F_N(x_N)). \tag{28}$$

Assume the Pearson correlation coefficient can be obtained from the historical data, the Gaussian copula function is used to obtain the correlated samples of power generations in ADN. The CDF of the Gaussian copula function can be expressed as:

$$C(u_1, u_2, \cdots, u_N; \rho) = \varphi_\rho(\varphi^{-1}(u_1), \varphi^{-1}(u_2), \cdots, \varphi^{-1}(u_N)), \tag{29}$$

where ρ is the Pearson correlation coefficient matrix; φ_ρ is the CDF of the standard multivariate Guassian distribution with correlation coefficient matrix ρ and φ^{-1} is the inverse CDF of standard univariate Guassian distribution.

Provided that the marginal CDF of each renewable power generation and ρ are available, the steps to obtain the joint cumulants of the renewable power generation are as follows:

step 1: Obtain the CDF of the Gaussian copula function φ_ρ.

step 2: With the help of Gibbs sampling technique [18], obtain the samples of the Gaussian copula distribution $\boldsymbol{C}_{N\times M} = [\boldsymbol{c}_1, \boldsymbol{c}_2, \cdots, \boldsymbol{c}_M]$, where N is the number of sample and M is the dimension of variable.

step 3: Obtain the correlated samples $\boldsymbol{X}_{N\times M} = [\boldsymbol{x}_1, \boldsymbol{x}_2, \cdots, \boldsymbol{x}_M]$ with the $\boldsymbol{C}_{N\times M}$ and the marginal CDF of each renewable power generation F_j:

$$\boldsymbol{x}_i = F_i^{-1}(\boldsymbol{c_i}), \quad i = 1, 2, \cdots, M. \tag{30}$$

step 4: Obtain the joint moments of the renewable power generations based on the correlated samples $\boldsymbol{x}_{\cdot i} = [x_{1i}, x_{2i}, \cdots, x_{Ni}]^{\mathrm{T}}$:

$$a_{v,\boldsymbol{x}_i} = \sum_{j=1}^{N} (x_{ji})^v / N, v = 1, 2, \cdots. \tag{31}$$

step 5: Obtain the joint cumulants of the renewable power generations using the relationship between moments and cumulants [15].

As for the uncertain loads in ADN, since the normal distribution is used to describe their uncertainty, their cumulants can be calculated by:

$$\gamma^{(1)} = \mu, \gamma^{(2)} = \sigma^2, \gamma^{(v)} = 0 \quad \text{for} \quad v \geq 3 \tag{32}$$

E. PEMM for ADN

Figure 2 shows the flowchart of the PEMM to establish the probabilistic equivalent model of ADN. Because the PEMM only rely on the data available for the ADN, the probabilistic equivalent model can be constructed by the DSOs independently. This is helpful under the scenario that TSOs and DSOs function independently. With the help of the probabilistic equivalent model, TSOs can evaluate the impact of renewable power generation for the transmission system without knowing the detailed model of ADN. Thus, PEMM can be used to protect the commercially sensitive information and to help TSOs and DSOs collaborate in a secure and economic manner.

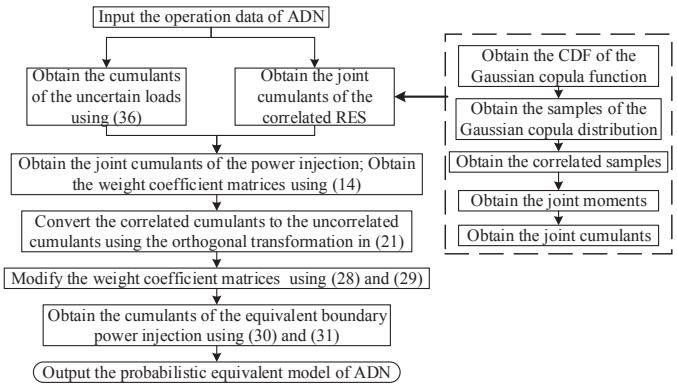

Fig. 2. The flowchart of PEMM for ADN.

IV. Case Studies

To demonstrate the effectiveness of the proposed method, simulations are taken on a CTDS. The transmission side of this CTDS is the modified IEEE 30-bus system shown in Fig. 3 and the detailed parameters of this system can be referred to [19]. The distribution side of this CTDS is based on the modified IEEE 34-bus system shown in Fig. 1 and the detailed parameters of this system can be found in [20]. The voltage bases of the transmission system and the ADN is 135 kV and 24.9 kV, respectively. The ADN is connected to the transmission system through bus 20 in the transmission system, which is regarded as the boundary bus.

The ADN incorporates six wind farms (WF) and four PV plants and the installed node and the capacities of them is shown in Table I. The v_{ci}, v_{co}, and v_{N} of wind turbines in these six wind farm are the 2 m/s, 14 m/s, and 11 m/s, respectively. The power factor of the wind farm is 0.98 (lagging). The shape parameter of the distribution of wind speed is 2.4 and the scale parameter is 7. With respect to PV plants, the parameters of the distribution of active power output are 0.52 and 2.6, respectively. For the uncertain loads in ADN, the expected value and the standard deviation is included in [20].

The correlation of wind speeds among the six wind farms is considered, so is the correlation of solar irradiances among four PV plants. The correlation coefficients for the wind speeds or the solar irradiances within the same node are relatively high. The Pearson correlation coefficient matrices for the wind speeds in the wind farms and for the solar irradiances in four PV plants are as follows:

$$\boldsymbol{\rho}_{\text{wind}} = \begin{bmatrix} 1 & 0.9 & 0.6 & 0.6 & 0.4 & 0.4 \\ 0.9 & 1 & 0.6 & 0.6 & 0.4 & 0.4 \\ 0.6 & 0.6 & 1 & 0.9 & 0.5 & 0.5 \\ 0.6 & 0.6 & 0.9 & 1 & 0.5 & 0.5 \\ 0.4 & 0.4 & 0.5 & 0.5 & 1 & 0.9 \\ 0.4 & 0.4 & 0.5 & 0.5 & 0.9 & 1 \end{bmatrix},$$

$$\boldsymbol{\rho}_{\text{PV}} = \begin{bmatrix} 1 & 0.9 & 0.5 & 0.5 \\ 0.9 & 1 & 0.5 & 0.5 \\ 0.5 & 0.5 & 1 & 0.9 \\ 0.5 & 0.5 & 0.9 & 1 \end{bmatrix}.$$

A. Verification of the Sampling Method Using the Gaussian Copula Function

In this case, to verify the effectiveness of the proposed sampling method, the wind speed samples of two wind farms in node 4 of ADN obtained from the proposed sampling method are compared with the predefined Weibull distribution. It is noted that there are two wind farms in node 4, the Person correlation coefficient of the wind speeds among them is 0.9 and the number of samples is 10000.

TABLE I
Configuration of RES generation units

Node	4	9	13	17	34
Type and number of RES	WF, 2	WF, 2	PV, 2	PV, 2	WF, 2
Capacity per RES (MW)	0.2	0.2	0.1	0.1	0.2

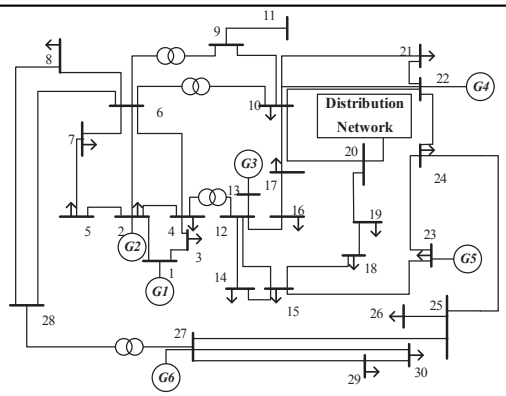

Fig. 3. The modified IEEE 30-bus power system with ADN integrated.

Kolmogorov-Smirnov test [21] is conducted to test whether the samples are drawn from the predefined distribution. In this case, the result of Kolmogorov-Smirnov test failed to reject the null hypothesis that the samples generated by our proposed sampling method come from the predefined Weibull distribution at the 1% significance level with the asymptotic p-value 0.8228. Moreover, the correlation coefficients for the wind speed samples of the two wind farms in node 4 is 0.898, which is pretty close to the predefined value 0.9. Hence, the results verify the proposed sampling method using the copula function can generate satisfactory correlated samples.

Table II shows the cumulants of the total wind power generation in node 4 of ADN from the proposed sampling method, which is denoted as S1, and from the independent sampling method, which is denoted as S2. We can see the cumulants from S1 are much larger than the those from S2 except the first order cumulants. Since the first order cumulant is the expected value and the second order cumulant is the variance, the results in Table II indicates that the wind power generation samples from S1 are more variant than those from S2. This result is consistent with the positively correlated nature of the wind speeds of these two farms.

TABLE II
The cumulants of power generation in node 4

	$\gamma^1_{P\text{g,wind}}/10^{-3}$	$\gamma^2_{P\text{g,wind}}/10^{-7}$	$\gamma^3_{P\text{g,wind}}/10^{-10}$
S1	1.38	6.63	1.01
S2	1.37	3.56	0.30
	$\gamma^4_{P\text{g,wind}}/10^{-13}$	$\gamma^5_{P\text{g,wind}}/10^{-16}$	$\gamma^6_{P\text{g,wind}}/10^{-19}$
S1	-3.37	-3.19	9.01
S2	-0.51	-0.22	0.31

B. Evaluation of the Probabilistic Equivalent Model Using the Cumulant Based Probabilistic Load Flow

Probabilistic load flow (PLF) is an essential tool to analyze the states of power system considering the uncertainty.

Performing PLF on the probabilistic equivalent model and the original system, respectively, we can evaluate the accuracy of the probabilistic equivalent model by comparing the results from the equivalent model with those from the original system.

With the cumulants of the equivalent boundary power injection obtained from PEMM, the probabilistic equivalent model can be readily integrated into the cumulant based probabilistic load flow (CPLF) [22]. The equivalent boundary power injection can be regarded as an equivalent generator representing the ADN. Then CPLF can be performed on the probabilistic equivalent model and its detailed procedure is as follows [22]:

step 1: Compute the cumulants of the equivalent boundary power injection using PEMM.

step 2: Compute the cumulants of the power injections of other buses except for boundary bus according to the given probabilistic distribution.

step 3: Compute the cumulants of the state variables including voltage and branch flow according to the cumulants of the power injections and the linearized power flow equation.

step 4: Calculate the Gram-Charlier expansion coefficients of the state variables using the corresponding cumulants and obtain the CDF and PDF of the state variables.

In this case, the CPLF is run on the probabilistic equivalent model. For convenience, the probabilistic equivalent model obtained from the proposed PEMM is denoted as M1 while the probabilistic equivalent model obtained from the PEMM neglecting the correlation is denoted as M2. There are two differences between the M1 and the M2: one is that the M2 is derived from (17) and (18) whereas the M2 is derived from (24) and (25); the other is that the cumulants of the renewable power generation of M1 are obtained from S1 while those of M2 are obtained from S2. The results of the CPLF based on the original system are regards as the benchmarks.

The relative errors of the cumulants of state variables are regarded as the index of the accuracy:

$$\varepsilon^{v}_{m,s} = |(\gamma^{v}_{m,s} - \gamma^{v}_{s0})/\gamma^{v}_{s0}|, \tag{33}$$

where ε is the relative error; m is the index of equivalent model; s is the type of state variables, which includes the voltage magnitudes of PQ nodes, the voltage phase angle of PQ and PV nodes, the active and reactive power flow of branch and reactive power flow of branch; 0 represents the cumulants of the state variables of the original test system.

Fig. 4 through 6 depict the relative error index of the cumulants of the voltage magnitude, the active power flow of branch and the reactive power flow of branch, respectively. The errors of the first order cumulant of the state variables for both M1 and M2 are pretty small. Since the first order cumulant is the expect value of the variables, this result demonstrates the probabilistic equivalent model obtained from the PEMM can retain the consistency of the load flow under the basic operation condition. Moreover, the errors of the second order cumulant of the state variables for M1 is smaller than those of M2. The minor error in the second order cumulant verifies that M1 can capture the probabilistic characteristics and substantiate the effectiveness of PEMM. Besides, the comparison

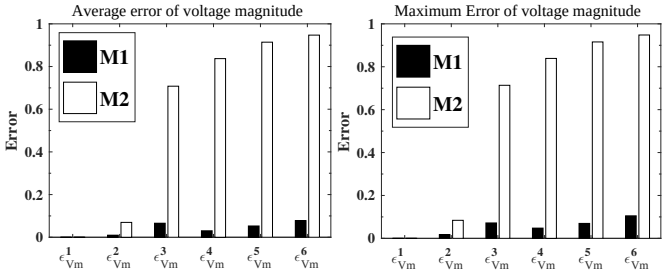

Fig. 4. The relative error index of the cumulants w.r.t. the voltage magnitude.

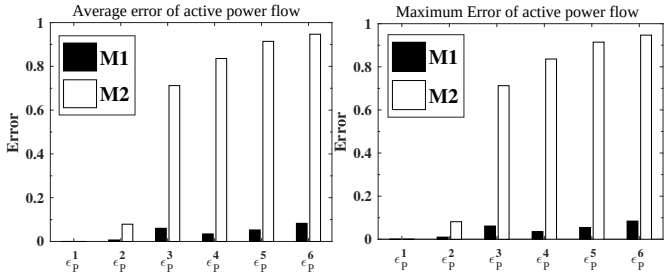

Fig. 5. The relative error index of the cumulants w.r.t. the active power flow.

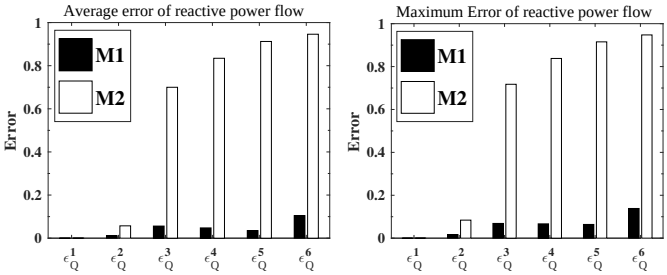

Fig. 6. The relative error index of the cumulants w.r.t. the reactive power flow.

results demonstrate the necessity of the consideration of the correlation of the distributed RES.

Furthermore, the errors of the higher-order cumulant of the state variables for M1 is much smaller than those of M2 and all the errors of M1 are less than 0.2. Hence, we can conclude that the results of CPLF based on the probabilistic equivalent model which is obtained from the proposed PEMM is pretty close to the results of CPLF based on the original test system. Besides, the consideration of the correlation between the RES can improve the accuracy of the probabilistic equivalent model.

The computation time of the CPLF based on the original test system is 1.821s while the computation time of CPLF based on M1 is 0.542s. Using the probabilistic equivalent model, the computation time is reduced by 70.2%. Thus, the efficiency of the analysis upon the transmission network with the CPLF can be enhanced much as well.

C. Evaluation of the Probabilistic Equivalent Model Using Monte Carlo Simulation Based PLF

To further demonstrate the effectiveness of the proposed PEMM and evaluate the accuracy of the probabilistic equivalence model, the Monte Carlo simulation based PLF (MCS-PLF) is run on the model M1 and M2, respectively. The results of the MCS-PLF which is run on the original test system are considered as benchmarks. The number of Monte-Carlo simulation is 10000.

MCS-PLF relies on the samples of variables and the deterministic load flow. The procedure of MCS-PLF using the probabilistic equivalent model is developed as follows:

step 1: Compute the cumulants of the equivalent boundary power injection using PEMM.

step 2: Calculate the Gram-Charlier expansion coefficients of the the equivalent boundary power injection using the corresponding cumulants and then obtain the CDF of the equivalent boundary power injection F_{eq}.

step 3: Generate the samples of the uniform distribution $U_M = [u_1, u_2, \cdots, u_M]$ and obtain the samples of the equivalent boundary power injection using the inverse CDF: $e_i = F_{\text{eq}}^{-(1}(u_i) \quad i = 1, 2, \cdots, M$

step 4: Run the deterministic load flow based on the samples of the equivalent boundary power injection.

step 5: Obtain the statistics of the state variables according to the results of the deterministic load flow.

The Bhattacharyya distance is used to measure the similarity of the probability distributions of the state variables, of which the type is the same as that in the CPLF. The Bhattacharyya distance is considered to a reliable index since it takes not only the means but also the standard deviations into account. Consequently, when two probability distributions have the same means but different standard deviations, the Bhattacharyya distance grows depending on the difference between the standard deviations [23], [24]. Hence, the Bhattacharyya distance between the probability distributions of the state variables of the probabilistic equivalent model and the original test system is applied to evaluate the accuracy of the probabilistic equivalent model.

Figs. 7 through 9 show the Bhattacharyya distances with respect to the voltage magnitude, the active power flow of branch and the reactive power flow of branch, respectively. The Bhattacharyya distances for branch flow of branch 13, 37, 38 and 39 are not shown because they are constants instead of variables in this case. In this case, the Bhattacharyya distances are small, which can verify the equivalent model can capture the probabilistic characteristics of ADN and the probabilistic equivalent model can be incorporated into MCS-PLF successfully.

All the Bhattacharyya distances between the state variables of M1 and the state variables of the original test system are smaller than those between the state variables of M2 and the state variables of the original test system. Thus, the figures also demonstrate that considering the correlation of RES is necessary and can improve the accuracy of the probabilistic equivalent model.

Figs. 10 through 12 show the PDF curves of some state variables of the M1, the M2 and the original test system, respectively. These state variables are selected from the buses or branches which are close to the boundary bus. Hence, they are more likely to be affected by the equivalent model and are suitable to be used to evaluate the performance of the equivalent model. Compared with the M2 curves, the M1 curves are closer to the original curves than the M2 curves, which can further substantiate the conclusion we draw in the last paragraph.

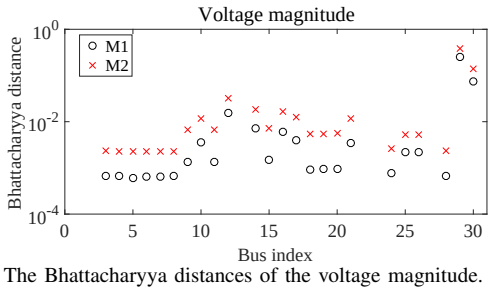

Fig. 7. The Bhattacharyya distances of the voltage magnitude.

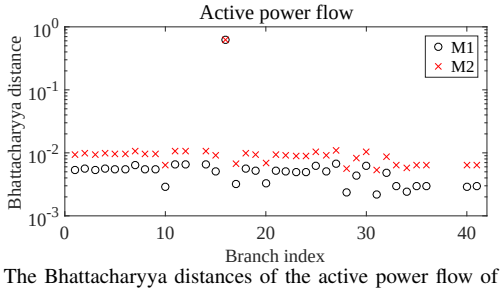

Fig. 8. The Bhattacharyya distances of the active power flow of branch.

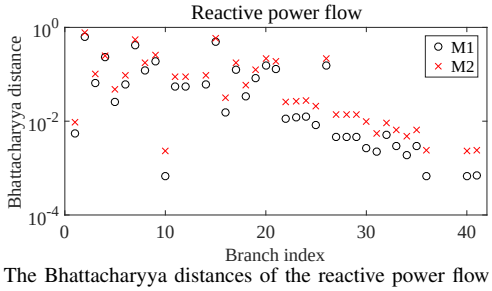

Fig. 9. The Bhattacharyya distances of the reactive power flow of branch.

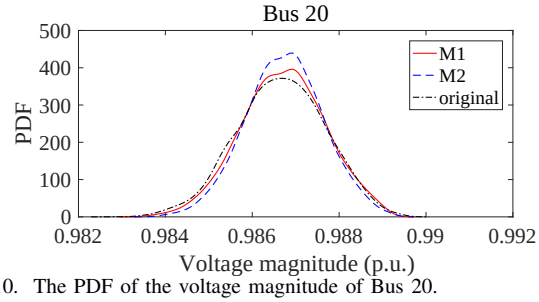

Fig. 10. The PDF of the voltage magnitude of Bus 20.

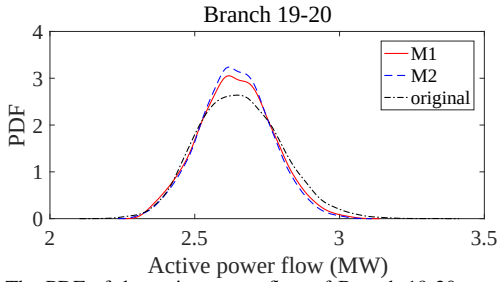

Fig. 11. The PDF of the active power flow of Branch 19-20.

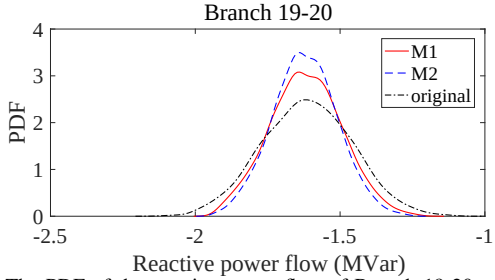

Fig. 12. The PDF of the reactive power flow of Branch 19-20.

The computation time of the MCS-PLF based on the original test system is 53.15s while the computation time of MCS-PLF based on M1 is 15.34s. Using the probabilistic equivalent model, the computation time is reduced by approximately 71.1%. Hence, the efficiency of the analysis upon the transmission network with the MCS-PLF can be enhanced much.

V. Conclusions and future work

A probabilistic equivalent modeling method (PEMM) for ADN considering the uncertainty of RES is proposed in this paper. The mathematical formulation of the PEMM is investigated and extended to take the correlation of RES into account. Moreover, as the source of input data for PEMM, a sampling method which is based on the Gaussian copula function is developed to formulate the correlation of RES and to generate the correlated renewable power generation samples and cumulants. The results of case studies support the following conclusions: 1. the results of the Kolmogorov-Smirnov test and the assessment of the correlation coefficient verify the effectiveness and the practicality of the proposed sampling method; 2. the simulation studies based on CPLF and MCS-PLF demonstrate that the results of PLF using the probabilistic equivalent model is pretty close to those using the original model. Moreover, the comparative results concerning the correlation of RES substantiate that the consideration of correlation of RES can enhance the accuracy of the equivalent model; 3. the comparative results on computation time demonstrate using the PEMM can reduce the computation time by approximately 70% while keeping the high accuracy, thereby enhancing the efficiency of the analysis of the transmission network.

The proposed PEMM could be used to provide the equivalent model for the applications on the transmission network in which should consider the impact of RES, e.g., static security analysis, reliability assessment, economic dispatch, unit commitment, and optimal power flow. Besides, the proposed PEMM could be adopted in the separate operating environment to coordinate the operation of the transmission network and the distribution network. These issues could be further explored in future work.

References

[1] Y. Jiang, J. Xu, Y. Sun, C. Wei, J. Wang, S. Liao, D. Ke, X. Li, J. Yang, and X. Peng, "Coordinated operation of gas-electricity integrated distribution system with multi-cchp and distributed renewable energy sources," *Applied Energy*, vol. 211, pp. 237–248, 2018.

[2] S. M. Zali and J. V. Milanovi, "Generic model of active distribution network for large power system stability studies," *IEEE Trans. Power Syst.*, vol. 28, no. 3, pp. 3126–3133, 2013.

[3] H. Golpra, H. Seifi, and M. R. Haghifam, "Dynamic equivalencing of an active distribution network for large-scale power system frequency stability studies," *IET Generation Transmission & Distribution*, vol. 9, no. 15, pp. 2245–2254, 2015.

[4] A. Samadi, L. Sder, E. Shayesteh, and R. Eriksson, "Static equivalent of distribution grids with high penetration of pv systems," *IEEE Transactions on Smart Grid*, vol. 6, no. 4, pp. 1763–1774, 2015.

[5] M. G. Jeong, Y. J. Kim, S. I. Moon, and P. I. Hwang, "Optimal voltage control using an equivalent model of a low-voltage network accommodating inverter-interfaced distributed generators," *Energies*, vol. 10, no. 8, p. 1180, 2017.

[6] W. Dai, J. Yu, X. Liu, and W. Li, "Two-tier static equivalent method of active distribution networks considering sensitivity, power loss and static load characteristics," *International Journal of Electrical Power and Energy Systems*, vol. 100, pp. 193–200, 2018.

[7] A. C. Neto, A. B. Rodrigues, R. B. Prada, and M. Silva, "External equivalent for electric power distribution networks with radial topology," *IEEE Trans. Power Syst.*, vol. 23, no. 3, pp. 889–895, 2008.

[8] J. V. Milanovi and S. M. Zali, "Validation of equivalent dynamic model of active distribution network cell," *IEEE Trans. Power Syst.*, vol. 28, no. 3, pp. 2101–2110, 2013.

[9] A. Baziar and A. Kavousi-Fard, "Considering uncertainty in the optimal energy management of renewable micro-grids including storage devices," *Renewable Energy*, vol. 59, no. 6, pp. 158–166, 2013.

[10] Z. Xie, T. Ji, M. Li, and Q. Wu, "Quasi-monte carlo based probabilistic optimal power flow considering the correlation of wind speeds using copula function," *IEEE Trans. Power Syst.*, vol. 1, 2017.

[11] M. S. Li, Z. J. Lin, T. Y. Ji, and Q. H. Wu, "Risk constrained stochastic economic dispatch considering dependence of multiple wind farms using pair-copula," *Applied Energy*, vol. 226, pp. 967–978, 2018.

[12] J. Usaola, "Probabilistic load flow with wind production uncertainty using cumulants and cornishfisher expansion," *International Journal of Electrical Power & Energy Systems*, vol. 31, no. 9, pp. 474–481, 2009.

[13] K. P. Kumar and B. Saravanan, "Recent techniques to model uncertainties in power generation from renewable energy sources and loads in microgrids a review," *Renewable & Sustainable Energy Reviews*, vol. 71, pp. 348–358, 2016.

[14] J. M. Morales and J. Perez-Ruiz, "Point estimate schemes to solve the probabilistic power flow," *IEEE Trans. Power Syst.*, vol. 22, no. 4, pp. 1594–1601, 2007.

[15] M. G. Kendall *et al.*, "The advanced theory of statistics." *The advanced theory of statistics.*, no. 2nd Ed, 1946.

[16] J. M. Morales, L. Baringo, A. J. Conejo, and R. Minguez, "Probabilistic power flow with correlated wind sources," *IET Generation Transmission & Distribution*, vol. 4, no. 5, pp. 641–651, 2010.

[17] A. Sklar, "Random variables, joint distribution functions, and copulas," *Kybernetika -Praha-*, vol. 9, no. 6, pp. 449–460, 1973.

[18] J. Geweke, "Efficient simulation from the multivariate normal and student t-distributions subject to linear constraints," *Journal of Dermatologic Surgery & Oncology*, vol. 11, no. 4, p. 420423, 1992.

[19] R. W. Ferrero, S. M. Shahidehpour, and V. C. Ramesh, "Transaction analysis in deregulated power systems using game theory," *IEEE Trans. Power Syst.*, vol. 12(3), no. 3, pp. 1340–1347, 1997.

[20] R. M. Ciric, A. Padilha-Feltrin, and I. F. E. D. Denis, "Observing the performance of distribution systems with embedded generators," *International Transactions on Electrical Energy Systems*, vol. 14, no. 6, pp. 347–359, 2013.

[21] G. Marsaglia, W. W. Tsang, J. Wang, J. D. Leeuw, and A. Zeileis, "Evaluating kolmogorov's distribution," *Journal of Statistical Software*, vol. 08, no. i18, 2003.

[22] P. Zhang and S. T. Lee, "Probabilistic load flow computation using the method of combined cumulants and gram-charlier expansion," *IEEE Trans. Power Syst.*, vol. 19, no. 1, pp. 676–682, 2004.

[23] G. B. Coleman and H. C. Andrews, "Image segmentation by clustering," *Proceedings of the IEEE*, vol. 67, no. 5, pp. 773–785, 2005.

[24] F. Nielsen and S. Boltz, "The burbea-rao and bhattacharyya centroids," *IEEE Transactions on Information Theory*, vol. 57, no. 8, pp. 5455–5466, 2011.